Electronic Supplementary Information

The effect of hydroxyl group position on electrochemical reactivity and product selectivity of butanediol electro-oxidation

Shengnan Sun,[§a, b] Chencheng Dai,[§a] Libo Sun,[a] Zhi Wei Seh,[b] Yuanmiao Sun,[a] Adrian Fisher,[c] Xin Wang[d, e] and Zhichuan J. Xu*[a, e, f]

[a]School of Material Science and Engineering, Nanyang Technological University, 50 Nanyang Avenue, 639798 Singapore

[b]Institute of Materials Research and Engineering, Agency for Science, Technology and Research (A*STAR), 2 Fusionopolis Way, 138634 Singapore

[c]Department of Chemical Engineering and Biotechnology, University of Cambridge, West Cambridge Site, Philippa Fawcett Drive, CB3 0AS Cambridge, United Kingdom

[d]School of Chemical and Biomedical Engineering, Nanyang Technological University, 62 Nanyang Drive, Singapore 637459, Singapore

[e]Centre of Advanced Catalysis Science and Technology, Nanyang Technological University, 50 Nanyang Avenue, 639798 Singapore

[f]Energy Research Institute @ Nanyang Technological University, ERI@N, Interdisciplinary Graduate School, Nanyang Technological University, 50 Nanyang Avenue, 639798 Singapore

Email: xuzc@ntu.edu.sg

Experimental Procedures

Material preparation. Co_3O_4 electrodes were prepared by electrodepositing $Co(OH)_2$ on graphite paper and followed by annealing in air.[1] Firstly, $Co(OH)_2$ was electrodeposited on the graphite paper (1.0 cm × 1.0 cm) at -0.85 V vs. saturated calomel electrode (SCE) in 0.1 M $Co(NO_3)_2$ aqueous solution, keeping the passing 1.8 C at the room temperature. Then, the $Co(OH)_2$/graphite was transformed into Co_3O_4 by annealing at 300 °C in air for two hours. The mass loading of Co_3O_4 was ~1 mg. The crystal structure of electrode can be found in our previous report.[2]

Electrochemical measurements and other characterizations. The electrochemical tests were carried out by the three-electrode method with the as-prepared Co_3O_4 working electrode, a Hg/HgO (1 M KOH, aqueous) reference electrode and a Pt plate counter electrode (~1.0 cm × 3.0 cm) using a Bio-logic SP 150 potentiostat. Cyclic voltammetry (CV) measurements were performed to investigate and compare these diol compound oxidation reactions on Co_3O_4 from 0.824 to 1.524 vs. reversible hydrogen electrode (RHE) at 10 mV s^{-1} in 1.0M KOH solution. CV curves at 1 mV s^{-1} was used for Tafel plot. The diol compound oxidation potential was investigated and compared by means of CP in low current consecutively from 0.25, 0.50, 0.75 to 1.00 mA for 10 minutes, respectively. The scan rate effect was examined from 10, 20, 40, to 80 mV s^{-1}. The diol concentration mentioned above was kept at 0.75 M. Investigation of the diol compound concentration effect was performed by means of CP at 0.50 mA, diol concentrations increasing consecutively from 0.01 to 1.00 M. To analyze the diol oxidation products on Co_3O_4, the electro-oxidation experiment is carried out in 1.0 M KOH electrolyte at 1.524 V vs. RHE (nearby OER region) for 16 hours. To prevent the reduction of oxidation products at Pt counter electrode, the working and counter electrodes are separated by an anion exchange membrane in H-typed cell. Each chamber was filled with 10 mL of 0.75 M diol & 1 M KOH solution separated by an AMI-7001 anion exchange membrane, with Ar bubbling to purge air before and during experiments. The anolyte was analyzed after electrolysis using both HPLC and NMR methods. The conversion between the potentials vs. RHE and vs. Hg/HgO was performed by the following equation: E (vs. RHE) = E (vs. Hg/HgO) + $E_{Hg/HgO}$ (vs. SHE) + 0.059 × pH. $E_{Hg/HgO}$ (vs. SHE) = 0.098 vs. SHE at 25°C.

Product anslysis. Chromatographic determination of glycerol oxidation products was analyzed by an Agilent 1260 Infinity II HPLC (Agilent Technologies) using the method in our previous report.[3] The column used was an Aminex HPX87-H (Bio-Rad) and the eluent used was 5 mM sulfuric acid. During the test, 20 μL mixture of sample solution was injected into the column and the temperature of the column was kept at 60 °C. The flow rate was 0.5 mL/min. The separated compounds were detected with a refractive index detector (RID) and a multiple wavelength detector (MWD). The expected products were also analyzed by HPLC to perform a standard calibration curve. Both ^{1}H-NMR and ^{13}C-NMR spectrum were recorded using a Bruker AV 300 MHz NMR spectrometer. 0.4 mL sample and 0.1 mL D_2O were mixed and used for each test.

Calculation method. The first-principle calculations were performed with the Vienna Ab initio Simulation Package (VASP). The ion-electron interactions were treated with the projected-augmented wave (PAW) method.

The exchange-correlation interactions were calculated with the Perdew-Burke-Ernzehof (PBE) scheme. The energy cut-off was set to 400 eV, and the self-consistent convergence was set at criteria of 0.0001 eV/atom. The spin polarization was considered in the calculation. The GGA+U scheme was implemented, and the value of U_{eff} (U - J) for the Co-3d orbital is 4.3 eV. For the Co_3O_4-(111) surface structure, a 1×1 two-dimensional supercell consisting of four layers was constructed, which contains 48 Co atoms and 64 O atoms. The vacuum layer was set at more than 20.0 Å. The Norskov's computational hydrogen electrode (CHE) method was applied to calculate the reaction free energy (ΔG) for oxygen reduction reactions (ORR). In the method, with the standard conditions (pH=0, p = 1 bar, T = 298 K), the ΔG of the reaction: A* + H^++ e□→ AH*, could be calculated from the reaction: A* + 1/2H_2→AH*, i.e., ΔG= G (AH*) –G (1/2H_2) –G (A*) + eU. Here U is the electrode potential vs. SHE, and in alkaline condition, the formula between U' and U is U' = U + 0.059*(pH). In this work, U is not considered when comparing ΔG. The Bader charge was used analyze the charge density of the carbon atom.[4]

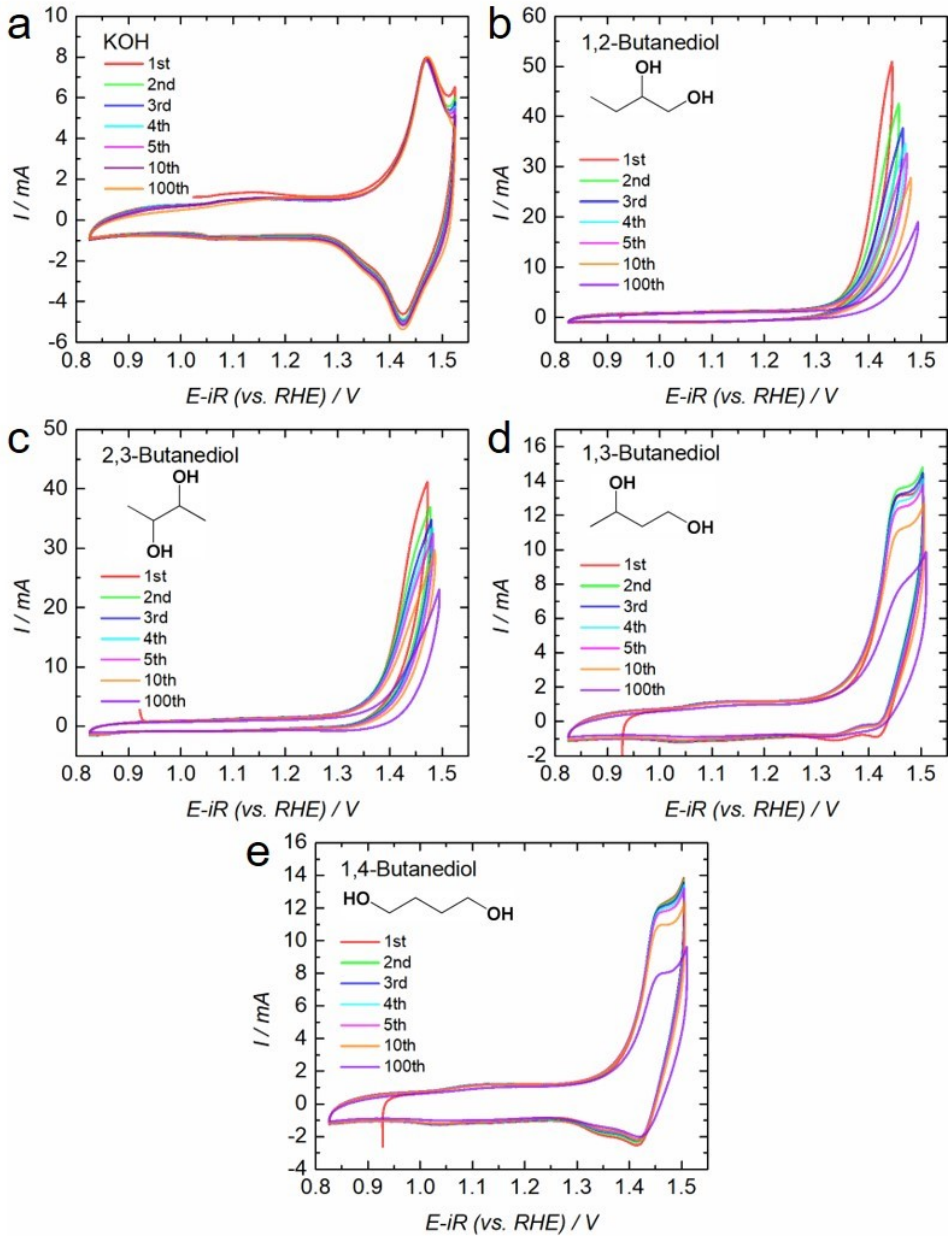

Fig. S1. The continuous CV cycles of Co_3O_4 in 1.0 M KOH in the absence (a) and the presence (b-e) of diols.

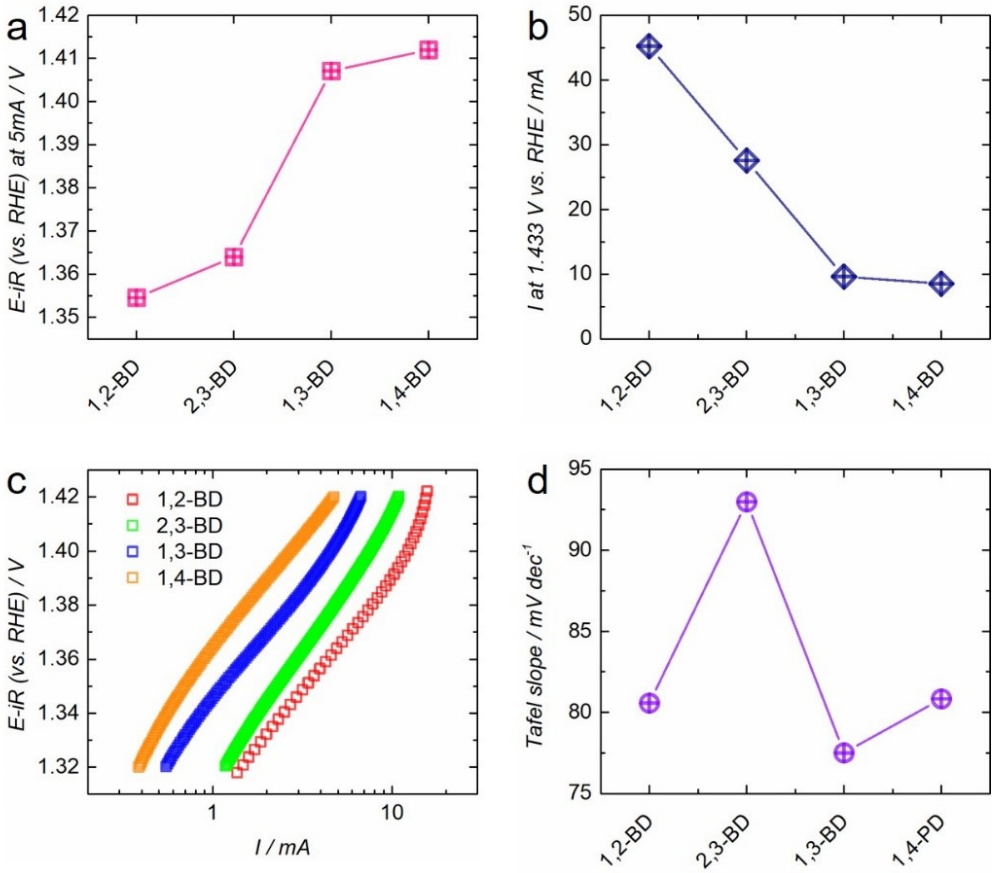

Fig. S2. (a) the diol oxidation potentials to reach a current of 5 mA higher than the background current (capacitance-corrected); (b) the diol oxidation currents at 1.433 V; (c) the Tafel slope in the anodic sweep of diol oxidation; (d) the Tafel slope derived from the anodic sweep of diol oxidation.

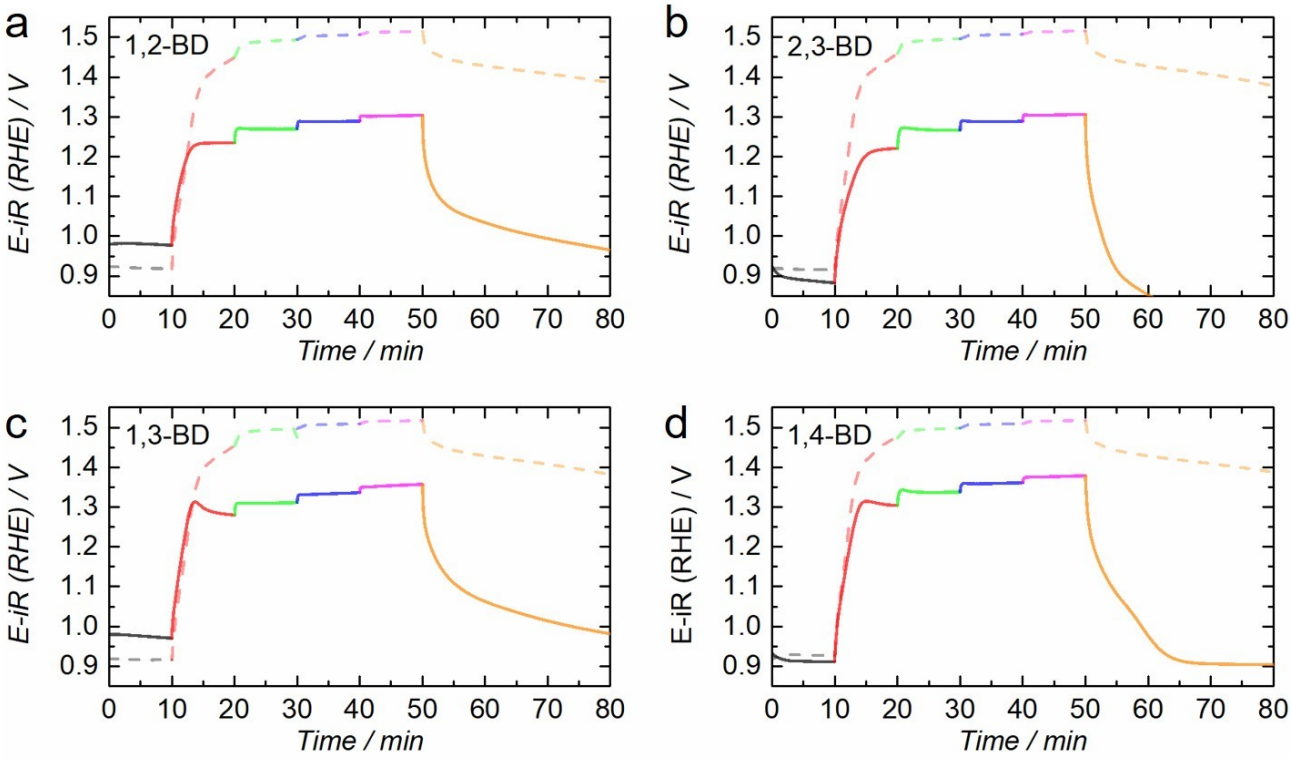

Fig. S3. CP curves of diol oxidation (solid line) and background (dash line) at different currents 0.25 mA (red line), 0.50 mA (green line), 0.75 mA (blue line), and 1.00 mA (magenta line).

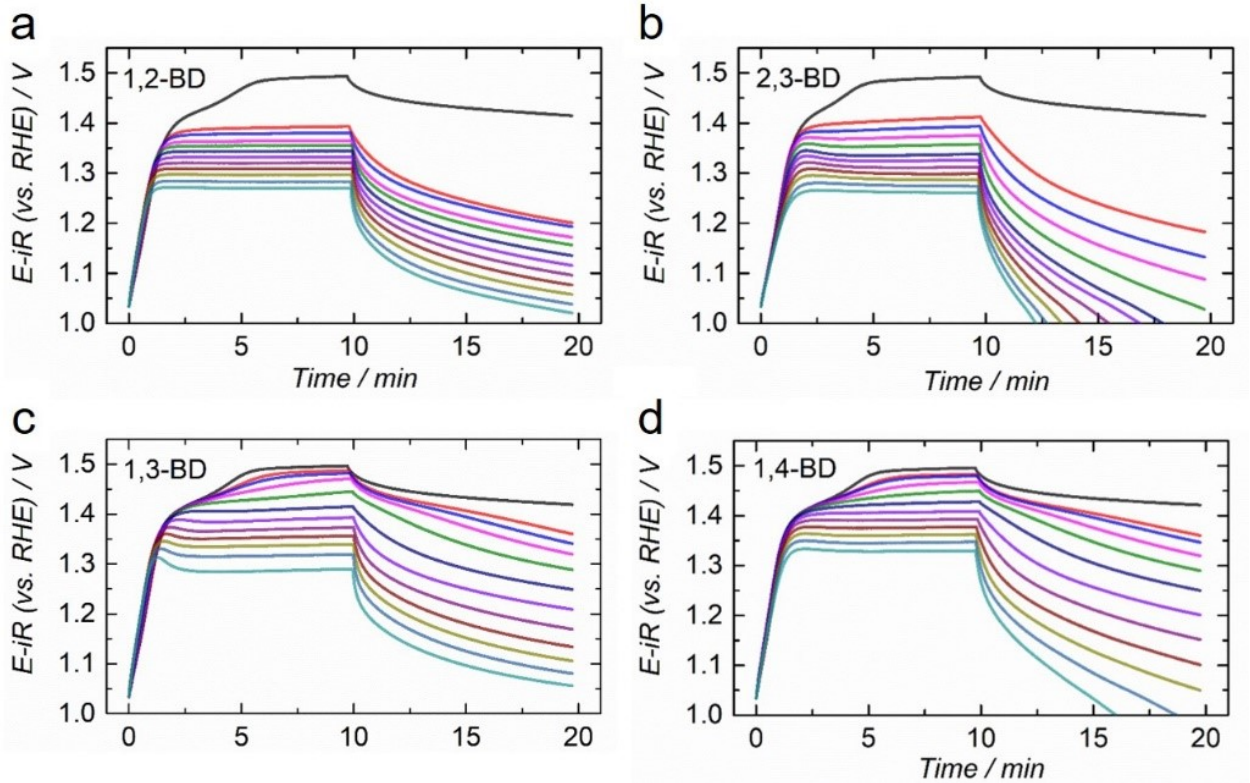

Fig. S4. CP curves with diol oxidation of different concentration (0, 0.01 ~ 1.00 M) and without diol (black line) at 0.50 mA.

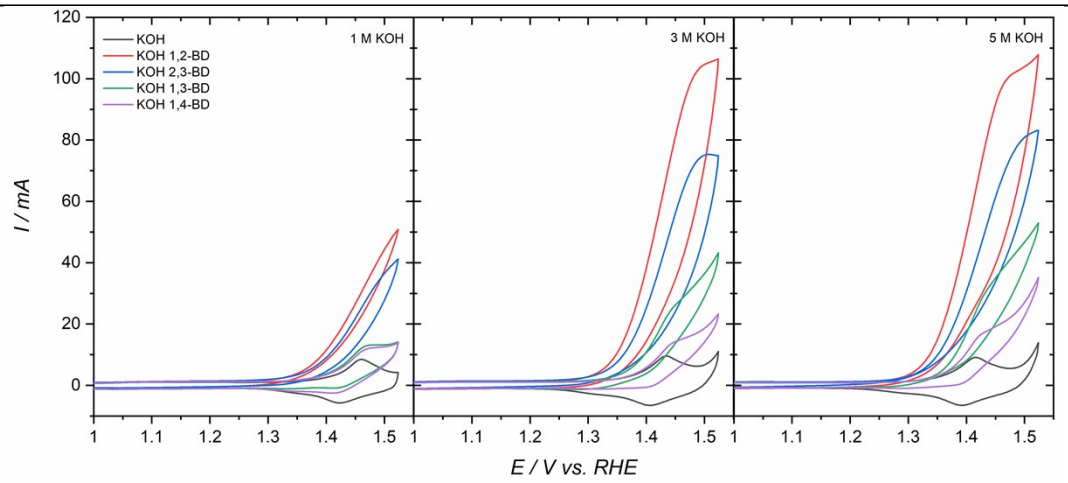

Fig. S5. The CV curves of 1,2-BD, 2,3-BD, 1,3-BD and 1,4-BD in the KOH solutions with different concentrations (1, 3, and 5 M). All butanediol electro-oxidation reactivity is enhanced by increasing the electrolyte pH.

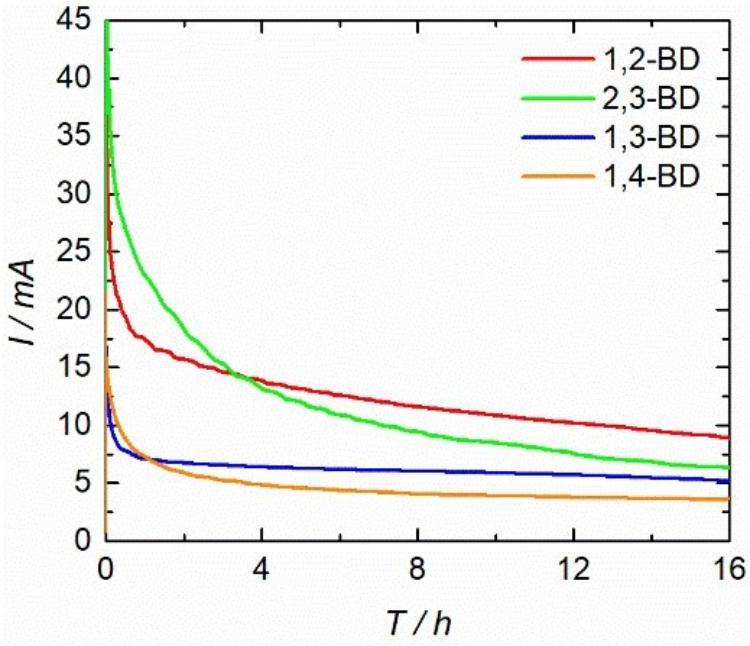

Fig. S6. The CA curves of electro-oxidation of various diols in 1 M KOH.

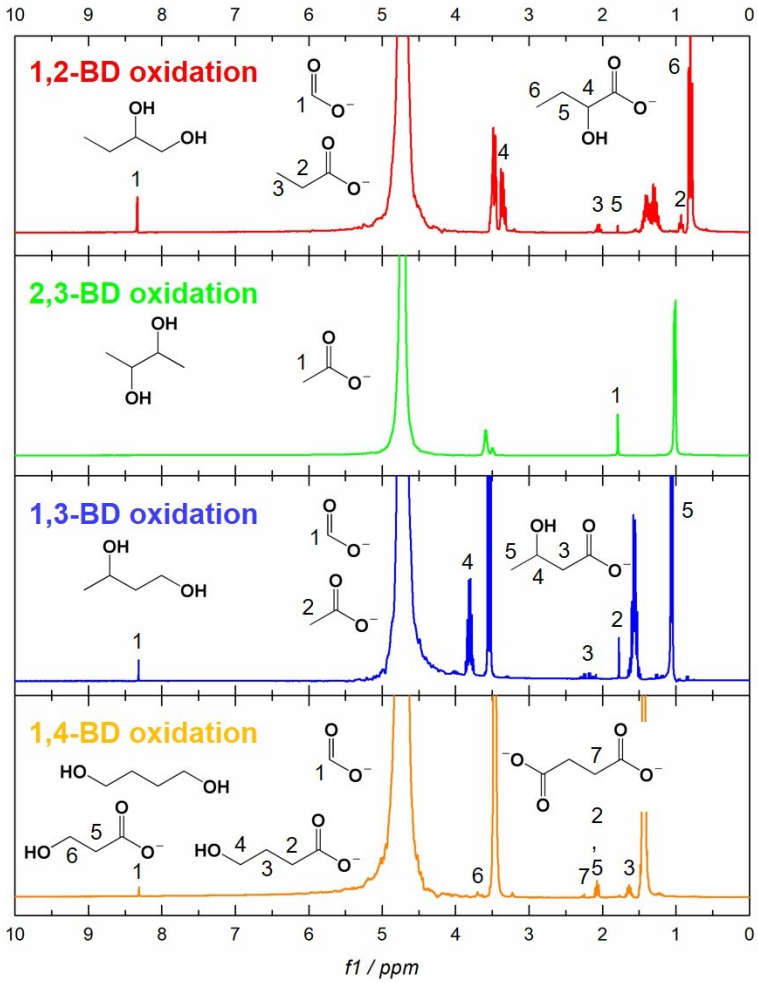

Fig. S7. ^{1}H NMR spectra of diol oxidation product electrolyte.

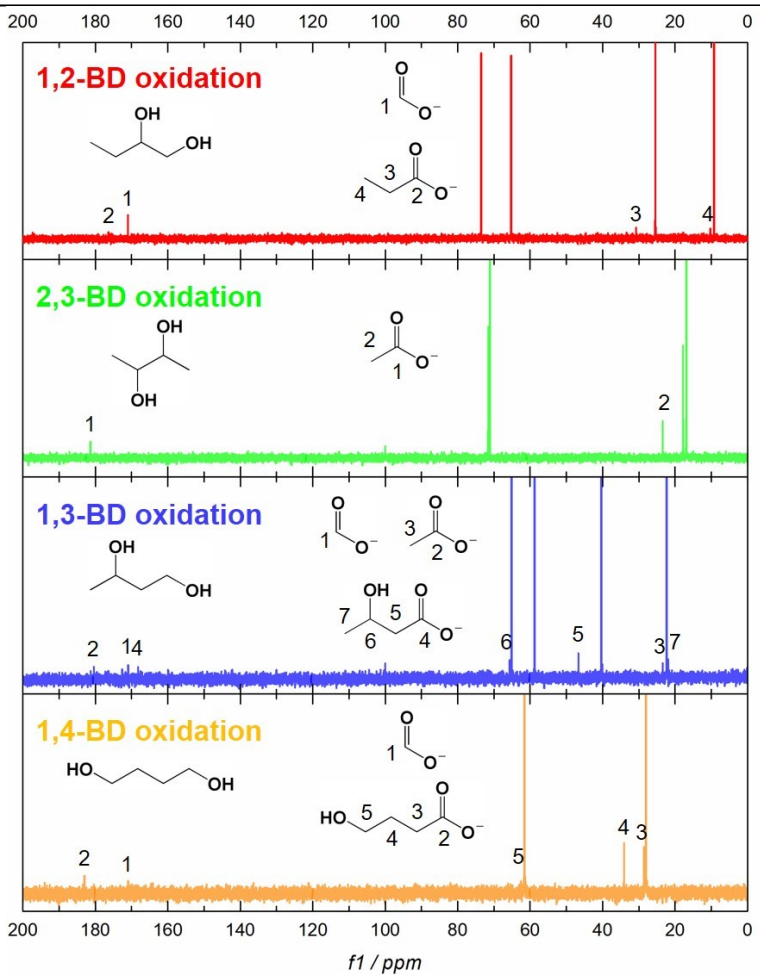

Fig. S8. ^{13}C NMR spectra of diol oxidation product electrolyte.

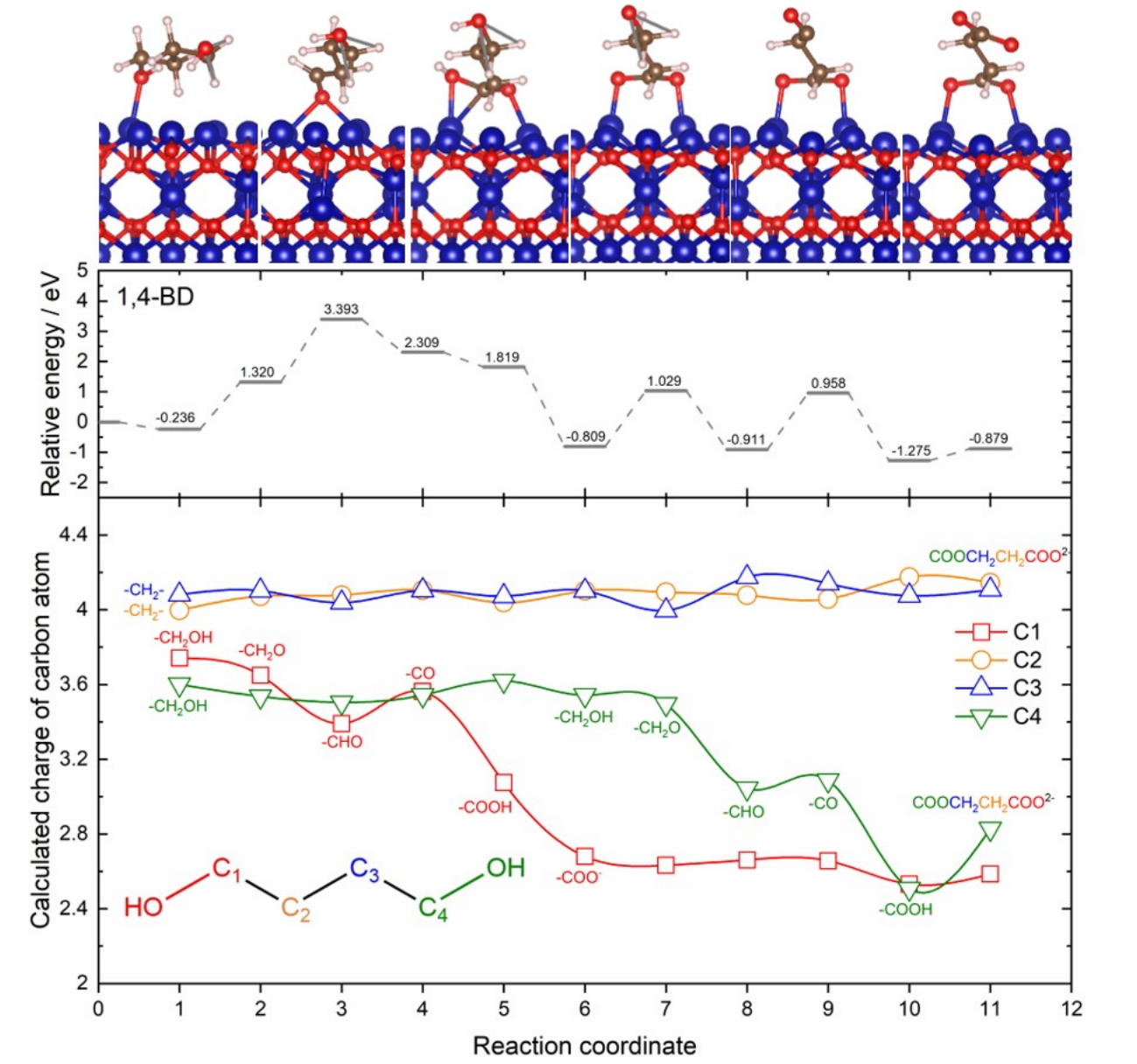

Fig. S9. The process of 1,4-BD electro-oxidation on the Co_3O_4 (111) surface for without C-C bond cleavage. (a) The representative illustration and adsorption energy of 1,4-BD; (b) the charge change of each carbon during oxidation.

Table S1. Elementary reaction steps of 1,2-BD electro-oxidation and relative free energy and variation of each step.

Step	Reaction	ΔG/ eV	G / eV
1	$CH_3CH_2CHOHCH_2OH + * \rightarrow CH_3CH_2CHOHCH_2OH*$	0.301	0.301
2	$CH_3CH_2CHOHCH_2OH + OH^- - e^- \rightarrow CH_3CH_2CHOHCH_2O + H_2O$	-0.194	0.108
3	$CH_3CH_2CHOHCHOH + OH^- - e^- \rightarrow CH_3CH_2CHOHCHO + H_2O$	1.114	1.222
4	$CH_3CH_2CHOHCOH + OH^- - e^- \rightarrow CH_3CH_2CHOHCO + H_2O$	1.269	2.491
5	$CH_3CH_2CHOHCO + OH^- - e^- \rightarrow CH_3CH_2CHOHCOOH$	-2.106	0.385
6	$CH_3CH_2CHOHCOOH + OH^- \rightarrow CH_3CH_2CHOHCOO^- + H_2O$	-1.471	-1.086
7	$CH_3CH_2CHOHCOO^- + OH^- - e^- \rightarrow CH_3CH_2COHCOO^- + H_2O$	1.203	0.118
8	$CH_3CH_2COHCOO^- + OH^- - e^- \rightarrow CH_3CH_2C(OH)_2COO^-$	-1.055	-0.937
9	$CH_3CH_2C(OH)_2COO^- \rightarrow HCOO^- + CH_3CH_2COOH$	0.018	-0.919

Note. * is not be written from Step 2.

Table S2. Elementary reaction steps of 2,3-BD electro-oxidation and relative free energy and variation of each step.

Step	Reaction	ΔG / eV	G / eV
1	$CH_3CHOHCHOHCH_3 + * \rightarrow CH_3CHOHCHOHCH_3*$	-0.088	-0.088
2	$CH_3CHOHCHOHCH_3* + OH^- - e^- \rightarrow CH_3CHOCHOHCH_3* + H_2O^-$	1.720	1.633
3	$CH_3CHOCHOHCH_3* + OH^- - e^- \rightarrow CH_3CHOCOHCH_3*+ H_2O$	-0.281	1.352
4	$CH_3CHOCOHCH_3* + OH^- - e^- \rightarrow CH_3CHOC(OH)_2CH_3*$	-1.009	0.343
5	$CH_3CHOC(OH)_2CH_3* \rightarrow CH_3CH_2O*+CH_3COOH$	-0.211	0.132
6	$CH_3COOH+ OH^-\rightarrow CH_3COO^- + H_2O$	-1.676	-1.543
7	$CH_3CH_2O* + OH^- - e^- \rightarrow CH_3CHO*+ H_2O$	0.473	-1.071
8	$CH_3CHO* + OH^- - e^- \rightarrow CH_3CO* + H_2O$	1.932	0.861
9	$CH_3CO* + OH^- - e^- \rightarrow CH_3COOH*$	-1.739	-0.877
10	$CH_3COOH*+ OH^-\rightarrow CH_3COO^-* + H_2O$	-1.279	-2.156
11	$CH_3COO^-* \rightarrow CH_3COO^- + *$	0.570	-1.587

Note. * is not be written from Step 2.

Table S3. Elementary reaction steps of 1,3-BD electro-oxidation and relative free energy and variation of each step.

Step	Reaction	ΔG / e	G / eV
1	$CH_3CHOHCH_2CH_2OH + * \rightarrow CH_3CHOHCH_2CH_2OH*$	-0.210	-0.210
2	$CH_3CHOHCH_2CH_2OH + OH^- - e^- \rightarrow CH_3CHOHCH_2CH_2O + H_2O$	0.274	0.064
3	$CH_3CHOHCH_2CH_2O + OH^- - e^- \rightarrow CH_3CHOHCH_2CHO + H_2O$	1.147	1.211
4	$CH_3CHOHCH_2CHO + OH^- - e^- \rightarrow CH_3CHOHCH_2CO + H_2O$	1.925	3.136
5	$CH_3CHOHCH_2CO + OH^- - e^- \rightarrow CH_3CHOHCH_2COOH$	-2.125	1.011
6	$CH_3CHOHCH_2COOH + OH^- \rightarrow CH_3CHOHCH_2COO^-$	-1.774	-0.762
7	$CH_3CHOHCH_2COO^- + OH^- - e^- \rightarrow CH_3COHCH_2COO^- + H_2O$	0.539	-0.223
8	$CH_3COHCH_2COO^- + OH^- - e^- \rightarrow CH_3COCH_2COO^- + H_2O$	0.183	-0.041
9	$CH_3COCH_2COO^- + OH^- - e^- \rightarrow CH_3COCHCOO^- + H_2O$	1.214	1.173
10	$CH_3COCHCOO^- + OH^- - e^- \rightarrow CH_3COCHOHCOO^-$	-0.372	0.802
11	$CH_3COCHOHCOO^- + OH^- - e^- \rightarrow CH_3COCHOCOO^- + H_2O$	1.521	2.323
12	$CH_3COCHOCOO^- + OH^- - e^- \rightarrow CH_3COCOCOO^- + H_2O$	-0.118	2.205
13	$CH_3COCOCOO^- + OH^- \rightarrow CH_3COOHCOCOO^{2-}$	1.187	3.392
14	$CH_3COOHCOCOO^{2-} \rightarrow CH_3COO^- + HCOCOO^-$	-2.899	0.493
15	$HCOCOO^- + OH^- \rightarrow HCOOHCOO^{2-}$	-0.619	-0.126
16	$HCOOHCOO^{2-} \rightarrow HCOO^- + HCOO^-$	-2.081	-2.208

Note. * is not be written from Step 2.

Table S4. Elementary reaction steps of 1,4-BD electro-oxidation and relative free energy and variation of each step.

Step	Reactant	G / eV	ΔG/ eV
1	$CH_2OHCH_2CH_2CH_2OH + * \rightarrow CH_2OHCH_2CH_2CH_2OH*$	-0.236	-0.236
2	$CH_2OHCH_2CH_2CH_2OH + OH^- - e^- \rightarrow CH_2OHCH_2CH_2CH_2O + H_2O$	1.555	1.320
3	$CH_2OHCH_2CH_2CH_2O + OH^- - e^- \rightarrow CH_2OHCH_2CH_2CHO + H_2O$	2.073	3.393
4	$CH_2OHCH_2CH_2CHO + OH^- - e^- \rightarrow CH_2OHCH_2CH_2CO + H_2O$	-1.083	2.309
5	$CH_2OHCH_2CH_2CO + OH^- - e^- \rightarrow CH_2OHCH_2CH_2COOH$	-0.490	1.819
6	$CH_2OHCH_2CH_2COOH + OH^- \rightarrow CH_2OHCH_2CH_2COO^- + H_2O$	-2.628	-0.809
Routine 1			
7_1	$CH_2OHCH_2CH_2COO^- + OH^- - e^- \rightarrow CH_2OHCH_2CHCOO^- + H_2O$	1.125	0.316
8_1	$CH_2OHCH_2CHCOO^- + OH^- - e^- \rightarrow CH_2OHCH_2CHOHCOO^- + H_2O$	-0.852	-0.536
9_1	$CH_2OHCH_2CHOHCOO^- + OH^- - e^- \rightarrow CH_2OHCH_2CHOCOO^- + H_2O$	1.920	1.384
10_1	$CH_2OHCH_2CHOCOO^- + OH^- - e^- \rightarrow CH_2OHCH_2COCOO^- + H_2O$	0.172	1.556
11_1	$CH_2OHCH_2CHOCOO^- + OH^- \rightarrow CH_2OHCH_2COOHCOO^{2-}$	-0.296	1.260
12_1	$CH_2OHCH_2COOHCOO^{2-} \rightarrow CH_2OHCH_2COO^- + HCOO^-$	-1.973	-0.713
Routine 2			
7_2	$CH_2OHCH_2CH_2COO^- + OH^- - e^- \rightarrow CH_2OCH_2CH_2COO^- + H_2O$	1.837	1.029
8_2	$CH_2OCH_2CH_2COO^- + OH^- - e^- \rightarrow CHOCH_2CH_2COO^- + H_2O$	-1.939	-0.911
9_2	$CHOCH_2CH_2COO^- + OH^- - e^- \rightarrow COCH_2CH_2COO^- + H_2O$	1.869	0.958
10_2	$COCH_2CH_2COO^- + OH^- - e^- \rightarrow COOHCH_2CH_2COO^-$	-2.234	-1.275
11_2	$COOHCH_2CH_2COO^- + OH^- \rightarrow COOCH_2CH_2COO^{2-} + H_2O$	0.396	-0.489

Note. * is not be written from Step 2.

References

[1] Sun, S; Sun, L.; Xi, S.; Du, Y.; Prathap, M. U. Anu.; Wang, Z.; Zhang, Q.; Fisher, A.; Xu, Z. J. Electrochemical oxidation of C3 saturated alcohols on Co_3O_4 in alkaline. *Electrochim. Acta*, **2017**, *228*, 183-194.

[2] Sun, S; Xu, Z. J. Composition dependence of methanol oxidation activity in nickel–cobalt hydroxides and oxides: an optimization toward highly active electrodes. *Electrochim. Acta*, **2015**, *165*, 56-66.

[3] Dai, C.; Sun, L.; Liao, H.; Khezri, B.; Webster, R. D.; Fisher, A. C.; Xu, Z. J. Electrochemical production of lactic acid from glycerol oxidation catalyzed by AuPt nanoparticles. *J. Catal.*, **2017**, *356*, 14-21.

[4] Henkelman, G.; Arnaldsson, A.; Jónsson, H. A fast and robust algorithm for Bader decomposition of charge density. *Comput. Mater. Sci.*, **2006**, *36*, 354-360.